Journal of Rock Mechanics and Geotechnical Engineering. 2009, 1 (1): 41–47

Journal of Rock Mechanics and Geotechnical Engineering

Journal online: www.rockgeotech.org

Mechanical properties of rock under coupled static-dynamic loads

Xibing Li[1,2], Zilong Zhou[1,2*], Fujun Zhao[1], Yujun Zuo[1], Chunde Ma[1], Zhouyuan Ye[1], Liang Hong[1]

[1] *School of Resources and Safety Engineering, Central South University, Changsha, 410083, China*

[2] *Hunan Key Laboratory of Resources Exploitation and Hazard Control for Deep Metal Mines, Central South University, Changsha, 410083, China*

Received 12 March 2009; received in revised form 16 May 2009; accepted 20 May 2009

Abstract: Rock drilling machine, INSTRON testing system, and SHPB device are updated to investigate the characteristics of rocks at great depth, with high loads from overburden, tectonic stresses and dynamic impacts due to blasting and boring. It is verified that these testing systems can be used to study the mechanical properties of rock material under coupled static and dynamic loading condition and give useful guidance for the deep mining and underground cavern excavation. Various tests to determine the rock strength, fragmentation behavior, and energy absorption were conducted using the updated testing systems. It is shown that under coupled static-dynamic loads, if the axial prestress is lower than its elastic limit, the rock strength is higher than the individual static or dynamic strength. At the same axial prestress, rock strength under coupled loads rises with the increasing strain rates. Under coupled static and dynamic loads, rock is observed to fail with tensile mode. While shear failure may exist if axial prestress is high enough. In addition, it is shown that the percentage of small particles increases with the increasing axial prestress and impact load based on the analysis of the particle-size distribution of fragments. It is also suggested that the energy absorption ratio of a specimen varies with coupled loads, and the maximum energy absorption ratio for a rock can be obtained with an appropriate combination of static and dynamic loads.

Key words: rock dynamic testing system; coupled static-dynamic loads; strength; fragmentation; energy absorption

1 Introduction

Since the establishment of the International Society for Rock Mechanics in Austria in 1962 [1–5], attentions have been paid to the study of the mechanical properties of rock material under different loading conditions through various testing systems. For example, INSTRON or MTS testing systems are employed to study the characteristics of rock material under static loading. SHPB (split Hopkinson pressure bar) and drop hammer are utilized to characterize the mechanical properties of rock material under dynamic load.

With the development of deep mining, high overburden underground cavern construction, as well as underground nuclear waste disposal, various abnormal phenomena in rock structure have been observed, such as large-scale zonal disintegration of rock masses, failure mode of rock mass from brittleness to ductility, and the exponential increment of rockburst accidents [6–11].

In fact, rocks at depths of several thousand meters can bear high static load from overburden and tectonic stresses, as well as the dynamic load induced from blasting and boring. For this case, studying the mechanical properties of rock material under static and dynamic loading separately may be not sufficient to depict the mechanism of the abnormal phenomena mentioned above.

In the present paper, different testing systems under coupled static-dynamic loads are introduced. By the testing systems, experimental works for rock material under coupled static-dynamic loads are conducted. The characteristics of rock material, such as the rock strength, fragmentation behavior, and energy absorption under different load conditions are presented.

2 Testing systems for rock under coupled static-dynamic loads

In order to provide useful and applicable testing systems under coupled static-dynamic loads, many exploratory trials and improvements have been undertaken for rock drilling machines, the INSTRON testing system and the SHPB device.

Doi: 10.3724/SP.J.1235.2009.00041
*Corresponding author. Tel: +86-731-8879612;
E-mail: zlzhou@mail.csu.edu.cn
Supported by the National Natural Science Foundation of China (10872218, 50934006, 50534030) and Research Foundation for the Doctoral Program of Higher Education of China (200805331143)

2.1 Rock testing system with a rock drilling machine

In 2001, a rock drilling machine was modified to conduct dynamic testing for rock material under static and dynamic loads. The system consists of a vertical loading device, a horizontal loading device, electric motors, a console, and a data acquisition unit, see Fig.1.

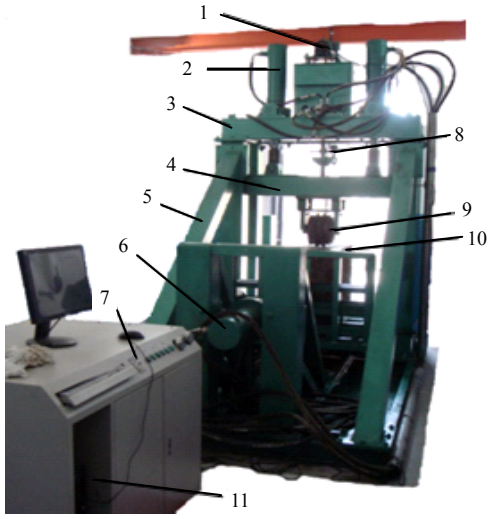

1–Speed control motor; 2–Vertical loading device; 3–Vertical loading device supporter; 4–Elevating beam; 5–Steel frame; 6–Horizontal loading device; 7– Console; 8–Impacting rod; 9–Cutter and cutter head; 10–Rock specimen; 11–Data acquisition unit.

Fig.1 Testing system for rock under combined loads.

The vertical loading device can impose combined static and dynamic loads on specimens simultaneously or separately. The static load is imposed by two hydraulic jacks connected with an elevating beam. The dynamic load is achieved by adjusting the speed of the electronic motor so that the impact velocity of a steel rod can be controlled. The horizontal loading device is mainly used to move the specimen back and forth freely; it also performs cutting force on rock specimens. With this system, rock failure under static load, impact load, and horizontal cutting can be observed. If the horizontal cutting force is absent or very low, the rock specimen is merely subjected to vertical static or dynamic load. If the vertical static force and horizontal cutting force are absent simultaneously, the system functions as a simple percussion drilling device.

The following working conditions are specified for this system. The static force varies from 0 to 440 kN. The impact energy on rock specimens varies from 0 to 100 J, with an impact frequency from 0 to 243 strokes per minute. The maximum horizontal cutting force can be 220 kN with a cutting speed of 60 mm/s.

Many trial tests were performed with this system to investigate the influences of cutter materials, the cutter's inclination angle, and combined loads on rock breakage efficiency. It was found that, under combined static and impact loads, the pitting depth and volume of broken rock increased with the increasing vertical static force and impact energy, while the specific energy of rock fragmentation decreased. By defining the appropriate ratio of static to impact forces as the minimum specific energy needed for rock fragmentation, the optimal efficiency for rock breakage can be determined. It is also shown that the breakage of soft rocks show higher sensitivity to cutting forces. With the increment of static force, the cutting depth and breaking efficiency of the cutter increase rapidly [12, 13].

This system can offer an effective tool for investigating cutter performance and rock fragmentation under combined static and dynamic loads. The results can be a good reference for choosing and optimizing a drilling machine and its accessories. However, the system only concerns about the breaking ability of rock by drilling tools, the dynamic deformation and strength properties of rock are difficult to determine. New experimental techniques should be further developed.

2.2 Rock testing system with an INSTRON testing machine

To obtain the constitutive relationship, failure pattern and other mechanical properties of rock under coupled loads, modifications were carried out on an INSTRON servo hydraulic material testing machine. With the actuator behind the loading discs, the static and disturbance loads can be applied to the specimens. At the same time, a new apparatus was constructed in the libratory to impose horizontal static pressure on specimens, see Fig.2.

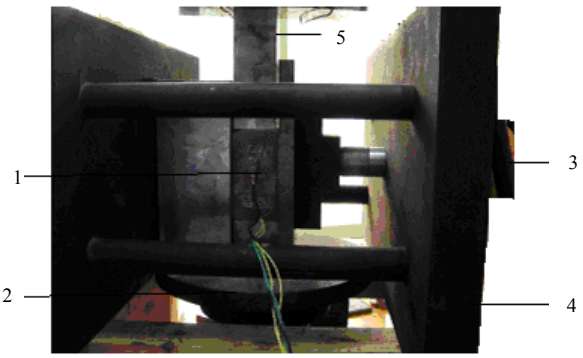

1–Specimen; 2–INSTRON actuator; 3–Oil pump; 4–Horizontal loading frame; 5–Loading transfer dummy

Fig.2 An apparatus producing horizontal static pressure on specimen.

Many siltstone specimens have been tested successfully with this system [14–16]. It is suggested that: (1) Under coupled loads, with an increment in static pressure, the strength and elastic modulus of rock first increased, and then decreased rapidly. Poisson's ratio decreased first and then increased. (2) Rock failure was mainly controlled by the static pressure. Under

hydrostatic stress states, it was difficult to break the rock, and the plasticity with shear was observed. (3) In elastic regions, the static load usually prevented the first fracture generation. Above elastic regions, static load accelerated the generation of first fractures. (4) Specimens failed with a double creep plane along the loading direction. With increased static pressure, the phenomenon was enhanced.

The testing system provides preliminary knowledge of rock behavior under coupled loads. However, as the actuator of the INSTRON system could only produce low-amplitude stress impulses with frequencies lower than several tens Hz, the stain rate of a specimen was less than 10^{-1} s^{-1}. This strain rate is much lower than those involved with practical engineering applications. For example, in drilling and blasting, rock is usually undertaken dynamic load at the strain rates larger than 10^{-1} s^{-1}. Therefore, the results obtained with the system are not sufficient to study the strain rate effect of rock materials. In addition, the disturbance produced by the INSTRON system is a harmonic wave, which induces fatigue in the specimens, resulting in the difficulty on the analysis of experimental results. Furthermore, the INSTRON system, traditionally used as static test machine, has been shown to give false results when the frequency of the harmonic wave is adequately high [17]. Therefore, a new method for rock tests under coupled loads should be further developed.

2.3 Rock testing system with an SHPB device

A new testing system, see Fig.3, based on the SHPB device has been designed to study the mechanical properties of rock material under coupled static and dynamic load. The system consists of a striker launcher, stress transmission components, an axial pre-compression stress inducer, a confining pressure inducer and a data acquisition unit. The striker launcher comprises the striker, gas tank, pressure vessels, gas switches and outlet valves. The stress transmission component is made up of two long elastic bars with 2 m in length and 50 mm in diameter. The specimen is sandwiched between the two elastic bars.

Fig.3 SHPB system for rock testing with coupled loads.

Surface-mounted strain gauges are glued to the middle of the elastic bars to measure strain histories induced by the stress waves propagating along the elastic bars. During the test, the axial prestress for rock specimen is applied through the pre-compression stress inducer. The impact load is controlled by varying the position of the striker in the gas tank.

With the SHPB system, rock specimens can be loaded with axial pre-compression stress of 0–200 MPa, confining pressures of 0–200 MPa and impact loads of 0–500 MPa, simultaneously or separately. The strain rate of the specimen can vary in the range of 10^{0}–10^{3} s^{-1}.

For testing rock-like brittle materials with the SHPB device, the key point is maintaining the load on specimens with specified constant strain rates. In a conventional SHPB device, a cylindrical striker produces rectangular stress waveforms in the input bar. However, many tests show that the rectangular input waveform is not suitable for tests of rock-like materials. This is because the increase of input load is so rapid that a specimen cannot experience constant strain rate during deformation, resulting in premature failure [4, 18–20]. For this case, a new purpose-built striker was used instead of the traditional cylindrical striker [4, 19, 21, 22]. This striker can produce a stress wave with a half-sine waveform. Figure 4 compares examples of signals produced by a traditional cylindrical striker and the new purpose-built striker.

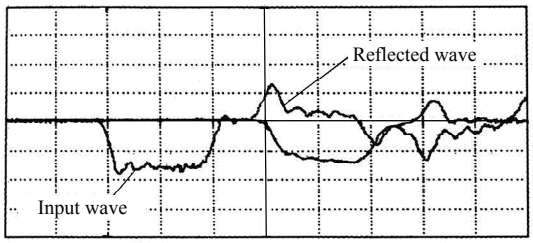

(a) Signal obtained with a traditional cylindrical striker.

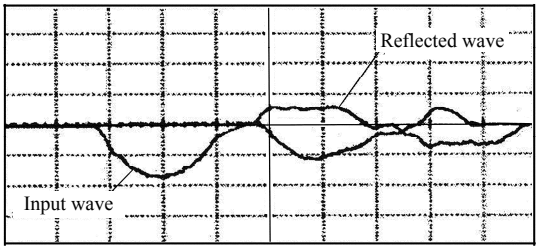

(b) Signals obtained with a purpose-built striker.

Fig.4 Signals obtained with two different strikers.

It can be seen that the reflected wave sourced by the purpose-built striker has long and smooth segments, whereas the reflected wave sourced by the traditional cylindrical striker has an apparent high-frequency

overprint that makes it much more rugged. According to the principle of the SHPB device, the reflected waveform indicates the strain rate of the specimen. Therefore, the purpose-built striker is better than the traditional cylindrical striker for testing brittle materials.

3 Strength characteristics of rock under coupled loads

With the newly-built SHPB testing system, the strength characteristics of siltstone specimens were investigated. The rock samples are almost homogeneous with average uniaxial compression strength of 90 MPa. The tests under coupled loads were conducted in two groups. In the first group, the peak stress applied by the impact load was kept constant, while the axial static prestress was varied over six levels. In the second group, the axial prestress was kept constant, while the impact load was varied over five levels. To account for possible scattering of the test results, the same tests were repeated for each of five specimens.

A typical test signal is shown in Fig.5. A flat segment can be found in the reflected wave, which shows the reliability of the signal.

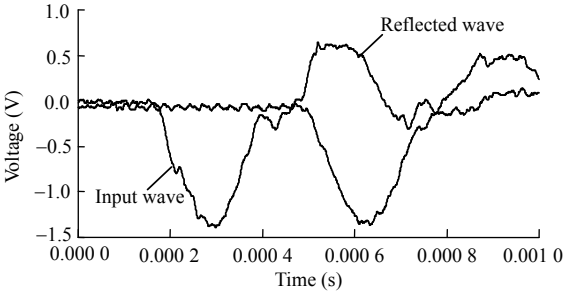

Fig.5 Typical testing signal with the new system.

3.1 Strength characteristics of rock under the same impact load but different prestresses

According to the uniaxial compression strength of the specimens, the prestress values were chosen as 18, 36, 45, 54, 72 and 81 MPa, which were equivalent to 20%, 40%, 50%, 60%, 80% and 90% of the static strength respectively.

Table 1 lists the related parameters of the specimens. Figure 6 shows the corresponding stress-strain curves. It should be noted that the test results of rock under an axial prestress of 63 MPa were so similar to the test results of rock under a prestress of 54 MPa, only one typical curve is shown in Fig.5.

It can be seen that the strength of siltstone increases greatly under coupled loads. The strength can be 120% higher than its uniaxial compression strength, or

Table 1 Related parameters of specimens.

Group No.	Set	Peak of impact load (MPa)	Axial prestress (MPa)	Diameter (mm)	Length (mm)	Density (kg/m^3)	Wave velocity (m/s)
I	1	200	18	49.42	26.84	2 430	3 576
	2	200	36	49.32	26.48	2 458	3 585
	3	200	45	49.28	26.34	2 480	3 620
	4	200	54	49.24	27.00	2 446	3 608
	5	200	72	49.18	26.28	2 520	3 584
	6	200	81	49.46	26.92	2 482	3 498
II	1	150	63	49.32	26.46	2 460	3 580
	2	200	63	49.44	26.28	2 620	3 654
	3	250	63	48.98	25.92	2 580	3 660
	4	300	63	49.20	26.40	2 684	3 620
	5	330	63	49.28	26.68	2 520	3 564

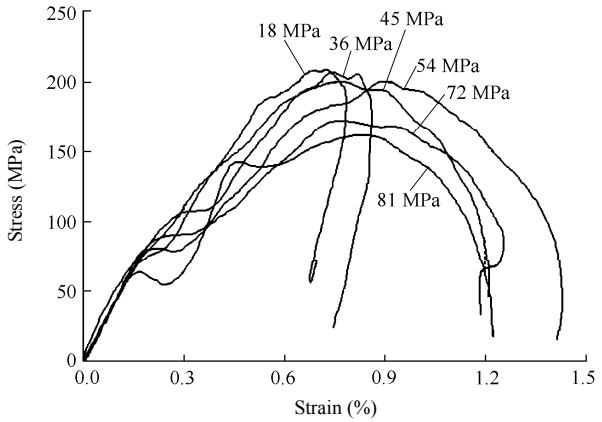

Fig.6 Stress-strain curves of siltstone under impact load of 200 MPa and different axial static prestresses.

30% higher than its dynamic strength. With the increase of axial prestress, the strength of the siltstone under coupled loads changed with the following trend.

(1) If the specimen was in an elastic deformation state under axial prestress, i.e. the prestress was less than 70% of the uniaxial compression strength of the specimen, the strength of the specimen under coupled loads would increase obviously and then remain constant unless the axial prestress exceeded the uniaxial compression strength of specimen. This may be due to the existing prestress and microcracks in rock material. Without prestress condition, microcracks, voids and fissures in rock will provide reflection surfaces for stress waves when the specimen is impacted. While with prestress, the defects in the specimen will be closed. The stress wave will travel through the specimen without reflecting. Therefore, a specimen should show higher strength under coupled loads.

(2) If the prestress exceeded the elastic limit of a specimen, i.e. the prestress was higher than 70% of the uniaxial strength of the specimen, the strength of rock under coupled loads would decrease abruptly. Actually, when the external stress exceeds the elastic limit of a

specimen, large numbers of microcracks appear due to internal damage. These microcracks provide reflection surfaces for successive impulses. The reflected tensile waves accelerate the crack occurrence, nucleation and congregation, which reduce the overall bearing capacity of specimen.

(3) When the prestress exceeded the yield limit of the specimen, i.e. the prestress reached almost 90% of the uniaxial compression strength of specimen, the measured stress-strain curve tended to be unstable. When rock is yielded, the failure of rock is critically vulnerable. Any slight disturbance would cause it to break into pieces. The critical behavior of a specimen affects the critical state of whole system. Upon impacting, the specimen structurally failed completely. As a result, the calculated stress-strain curve was rather oscillatory.

3.2 Strength characteristics of rock under the same prestress but different impact loads

Tests on siltstone under the same prestress but different impact loads were also conducted. The parameters for the typical specimens are listed in Table 1. As described in Section 3.1, it is known that (1) an appropriate prestress can enhance the strength of rock samples and (2) the strength will remain constant until the prestress exceeds the elastic limit. In these tests, a prestress of 63 MPa, a value close to elastic limit, was selected. The peak values of impact load were chosen to be 150, 200, 250, 300 and 330 MPa, respectively. Figure 7 shows the typical stress-strain curves.

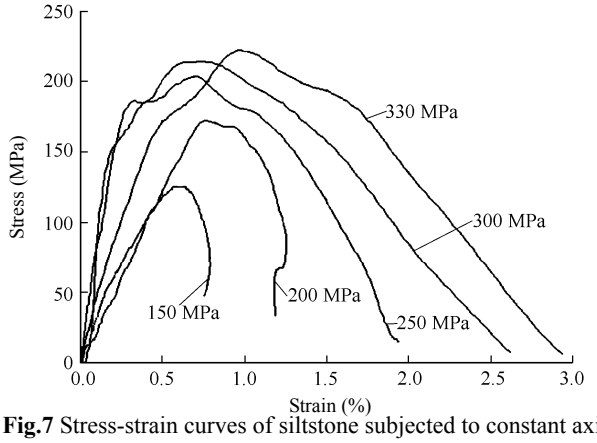

Fig.7 Stress-strain curves of siltstone subjected to constant axial prestress of 63 MPa but different impact loads.

Under the same prestress but different impact loads, the strengths of specimen under coupled loads are seen higher than that under uniaxial compression. The maximum increasing ratio of compressive strength may be 2.5 times higher. At the same time, it can be seen that the failure strengths of rock samples clearly increase with the increment of strain rate. When the peak stresses of the input wave are 150, 200, 250, 300 and 330 MPa, the strain rates of the specimen are 50, 80, 120, 150 and 180 s^{-1}, respectively, and the corresponding strength increment of the specimen under coupled loads are 30%, 90%, 120%, 130% and 145% of the uniaxial compressive strength, respectively.

4 Rock fragmentation under coupled loads

4.1 Failure pattern of rock under coupled loads

Rock failure is always caused by an interaction of microcracks. The failure pattern reflects the stress state of the rock directly. The observation of rock fracturing during the test showed three modes of specimen failure. (1) When the axial prestress was absent or very small, and the impact load was not very high, the specimen would break into two halves or several pieces, see Fig.8(a). (2) With the increase of impact load, the number of broken pieces increased, see Fig.8(b). (3) When the axial prestress and impact loads were both very high, the specimen would fail like a rockburst accompanied by a loud sound. Small fragments explosively flew from the apparatus, see Fig.8(c), where shear cones were found in the crumbling. From Figs.8(a) and (b), we can see that the failure pattern of rock under coupled loads is mainly tensile failure. While shear failure may exist if axial prestress is high enough.

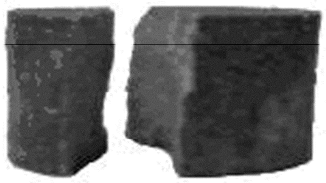

(a) Rock failure under small prestress and impact load.

(b) Rock failure under intermediate prestress and impact load.

(c) Rock failure under very high prestress and impact load or high impact load.

Fig.8 Rock failure patterns under different coupled loads.

4.2 Particle-size distribution of rock fragments under coupled loads

The particle-size distribution of rock fragments from the experiment reveals not only the failure state of a rock specimen but also the specific effect of loading conditions. Sieving statistics were collected for the specimen fragments using mesh sizes of 1, 2, 5, 10 and 20 mm. Each sieve fraction was then weighted. The accumulated percentage for a certain mesh size was calculated as the ratio of the weight of the passed fragments to the total weight of the specimen.

Figure 9 gives the results for group I. The accumulated percentage of particles is seen to increase with increasing axial prestress, indicating the axial prestress enhanced the rock fragmentation.

From the experimental results, it is suggested that, for mining at great depth, the high in-situ stress will help to improve the grade-size distribution of rock in drill and blast, secondary blasting or grinding are not needed to get good grade-size distribution.

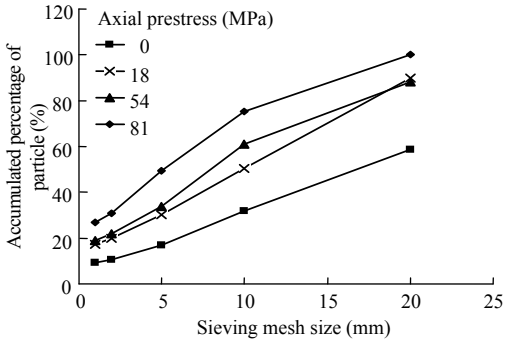

Fig.9 Particle-size distribution of specimens subjected to the same impact loading but different prestresses (group I).

Figure 10 gives the results from group II. It can be seen that the specimens become more fragmented with the increasing rock of impact load. For this case, in engineering practice, if there are too many large blocks or fine rock, the density of blasting holes and the amount of explosive in each hole should be increased to obtain the good grade-size distribution.

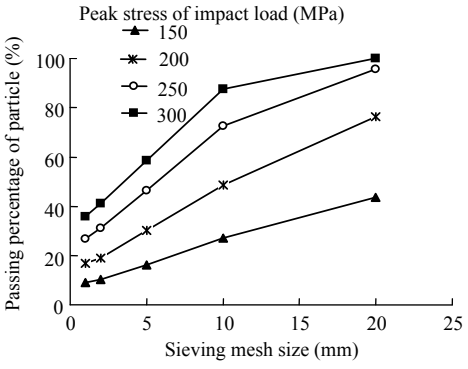

Fig.10 Particle-size distribution of specimens subjected to the same prestress but different impact loads (group II).

4.3 Energy absorption of rock under coupled loads

Based on wave theory and the SHPB principle, the input energy, reflected energy, and transmitted energy of a specimen (and their ratios) can be calculated [4, 23]. Figures 11 and 12 present the calculated results.

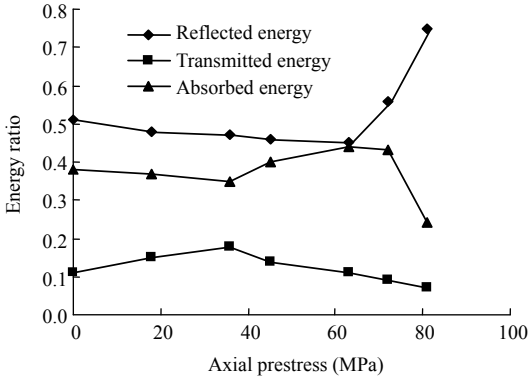

Fig.11 Energy absorption of rock failure under the same impact load but different axial prestresses.

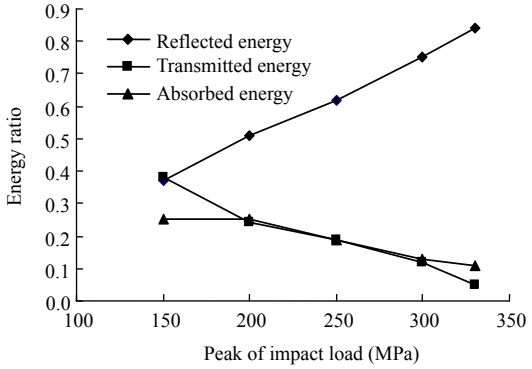

Fig.12 Energy absorption of rock failure under the same prestress but different impact loads.

It can be seen that, with constant impact loads and increasing axial prestresses, the reflected energy first decreases, and then increases, while the transmitted and absorbed energies increase first and then decrease. With constant prestress but increasing impact load, the reflected energy increases linearly, while transmitted and absorbed energies decrease gradually. Figure 11 also demonstrates that the absorbed energy ratio would reach the maximum value when the magnitude of the axial prestress is near the elastic limit of siltstone. The result indicates that appropriate prestress can improve the energy utilization ratio of drilling tools. This finding is of great importance to select and design the drilling machines in the deep mining.

5 Conclusions

Different testing systems under coupled static-dynamic loads are introduced in the present paper. Experimental works for rock material under coupled

static-dynamic loads through these testing systems are also conducted. It can be concluded that these testing systems can be available to study the mechanical properties of rock material under coupled static and dynamic loading condition and give useful guidance of the deep mining and underground cavern excavation.

It can be also concluded that the strengths of rock material under coupled static and dynamic loads are generally higher than the uniaxial static compression strength and dynamic strength under only impact loads. And also, under the same constant prestress, the compressive strengths clearly increase with the increasing strain rates. Under coupled static and dynamic loads, rock samples exhibit tensile failure modes and the fragmentation extent of rock increase with the increasing prestress and impact load.

It is also suggested that the appropriate coupling of static and dynamic loading can improve energy utilization efficiency in rock drilling and boring, and it can also improve the corresponding fragmentation effect of rock in the deep mining and underground cavern excavation.

References

[1] Hudson J A, Harrison J P. Engineering rock mechanics. Oxford: Elsevier Science Ltd., 1997.

[2] Sun J, Wang S. Rock mechanics and rock engineering in China: developments and current state-of-the-art. International Journal of Rock Mechanics and Mining Sciences, 2000, 37 (3): 447–465.

[3] Brown E T. Rock mechanics in Australia. International Journal of Rock Mechanics and Mining Sciences, 2002, 39 (5): 529–538.

[4] Li Xibing, Gu Desheng. Rock impact dynamics. Changsha: Central South University of Technology Press, 1994 (in Chinese).

[5] Cai Meifeng, He Manchao, Liu Dongyan. Rock mechanics and engineering. Beijing: Science Press, 2002 (in Chinese).

[6] Xie Heping. Resources development under high ground stress: present state, base science problems and perspective. In: The 175th Xiangshan Science Congress. Beijing: China Environmental Science Press, 2002: 179–191 (in Chinese).

[7] Feng Xiating. Several key rock mechanical problems in underground excavation and usage. In: The 175th Xiangshan Science Congress. Beijing: China Environmental Science Press, 2002: 192–201 (in Chinese).

[8] He Manchao, Lu Xiaojian, Jing Haihe. Characters of surrounding rockmass in deep engineering and its nonlinear dynamic mechanical design concept. Chinese Journal of Rock Mechanics and Engineering, 2002, 21 (8): 1 215–1 224 (in Chinese).

[9] Qian Qihu. The characteristic scientific phenomena of engineering response to deep rock mass and implication of deepnees. Journal of East China Institute of Technology, 2004, 27 (1): 1–5 (in Chinese).

[10] Malan D F, Basson F R. Ultra-deep mining: the increased potential for squeezing conditions. Journal of the South African Institute of Mining and Metallurgy, 1998, 98 (11/12): 353–363.

[11] Gu Desheng, Li Xibing. Modern mining science and technology for metal mineral researches. Beijing: China Metallurgical Industry Press, 2006 (in Chinese).

[12] Li X B, Zhao F J, Feng T, et al. A multifunctional testing device for rock fragmentation by combining cut with impact. Tunneling and Underground Space Technology, 2004, 19 (4/5): 526.

[13] Zhao Fujun, Li Xibing, Feng Tao, et al. Theoretical analysis and experiments of rock fragmentation under coupling dynamic and static loads. Chinese Journal of Rock Mechanics and Engineering, 2005, 24 (8): 1 315–1 321 (in Chinese).

[14] Li X B, Ma C D, Chen F, et al. Experimental study of dynamic response and failure behavior of rock under coupled static-dynamic loading. In: Proceedings of the ISRM International Symposium, the 3rd ARMS. Rotterdam: Mill Press, 2004: 891–895.

[15] Zuo Y J, Li X B, Zhou Z L, et al. Damage and failure rule of rock undergoing uniaxial compressive load and dynamic load. Journal of Center South University of Technology, 2005, 12 (6): 742–749.

[16] Li Xibing, Zuo Yujun, Ma Chunde. Failure criterion of strain energy density and catastrophe theory analysis of rock subjected to static-dynamic coupling loads. Chinese Journal of Rock Mechanics and Engineering, 2005, 24 (16): 2 814–2 825 (in Chinese).

[17] Bagde M N, Petroš V. The effect of machine behaviour and mechanical properties of intact sandstone under static and dynamic uniaxial cyclic loading. Rock Mechanics and Rock Engineering, 2005, 38 (1): 59–67.

[18] Li Xibing, Gu Desheng. On the reasonable loading stress waveforms determined by dynamic stress-strain curves of rocks by SHPB. Explosion and Shock Waves, 1993, 13 (2): 125–131 (in Chinese).

[19] Li X B, Lok T S, Zhao J. Oscillation elimination in the Hopkinson bar apparatus and resultant complete dynamic stress-strain curves for rocks. International Journal of Rock Mechanics and Mining Sciences, 2000, 37 (7): 1 055–1 060.

[20] Lok T S, Li X B, Liu D, et al. Testing and response of large diameter brittle materials subjected to high strain rate. Journal of Materials in Civil Engineering, ASCE, 2002, 14 (3): 262–269.

[21] Liu Deshun, Li Xibing, Zhu Pingyu. Dynamics and inverse design of impact machines. Beijing: Science Press, 2007 (in Chinese).

[22] Li Xibing, ZHOU Zilong, WANG Weihua. Construction of ideal striker for SHPB device based on FEM and neural network. Chinese Journal of Rock Mechanics and Engineering, 2005, 24 (23): 4 215–4 219 (in Chinese).

[23] Li X B, Lok T S, Zhao J. Dynamic characteristics of granite subjected to intermediate loading rate. Rock Mechanics and Rock Engineering, 2005, 38 (1): 21–39.